

Finite-Size Effect on Magnetic Ordering Temperatures in Long-Period Antiferromagnets: Holmium Thin Films

E. Weschke,* H. Ott, E. Schierle, C. Schüßler-Langeheine,† D.V. Vyalikh, and G. Kaindl
Institut für Experimentalphysik, Freie Universität Berlin, Arnimallee 14, D-14195 Berlin, Germany

V. Leiner,^{1,2} M. Ay,¹ T. Schmitte,¹ and H. Zabel¹

¹*Institut für Experimentalphysik/Festkörperphysik, Ruhr-Universität Bochum, D-44780 Bochum, Germany*
²*LSS, Institut Laue-Langevin, 38042 Grenoble Cedex, France*

P. J. Jensen

Institut für Theoretische Physik, Freie Universität Berlin, Arnimallee 14, D-14195 Berlin, Germany
(Received 21 January 2003; revised manuscript received 28 April 2004; published 5 October 2004)

The thickness dependence of the helical antiferromagnetic ordering temperature T_N was studied for thin Ho metal films by resonant magnetic soft x-ray and neutron diffraction. In contrast with the Curie temperature of ferromagnets, T_N was found to decrease with film thickness d according to $[T_N(\infty) - T_N(d)]/T_N(d) \propto (d - d_0)^{-\lambda'}$, where λ' is a phenomenological exponent and d_0 is of the order of the bulk magnetic period L_b . These observations are reproduced by mean-field calculations that suggest a linear relationship between d_0 and L_b in long-period antiferromagnets.

DOI: 10.1103/PhysRevLett.93.157204

PACS numbers: 75.25.+z, 75.70.Ak, 75.70.Cn

Reduced magnetic ordering temperatures are a well-known phenomenon of thin films [1–5]. This finite-size effect is caused by the reduced number of atoms in the direction perpendicular to the film plane that leads to a decrease of the total magnetic exchange energy. Reduced ordering temperatures have been observed for thin-film ferromagnetic (FM) systems, like Fe [1,6], Co [7], Ni [5,8], and Gd [9], and for antiferromagnetic (AFM) thin films of Cr in Cr/Fe multilayers [10,11] and CoO [12]. For the FM thin films, the thickness dependence of the Curie temperature T_C can be described by a power law of the form [2,4]

$$[T_C(\infty) - T_C(d)]/T_C(\infty) = C_0 d^{-\lambda}; \quad (1)$$

d is the film thickness, C_0 a constant, and $\lambda = 1/\nu$ is the so-called shift exponent, with ν the critical exponent of the magnetic correlation length. Although Eq. (1) is strictly valid only if d is much larger than a few monolayers (ML), it provides a reasonable description of experimental data down to rather small values of d [13]. For ultrathin films, deviations from Eq. (1) were observed and interpreted in terms of a spin-spin correlation length [13] or a transition to two-dimensional magnetism [8].

Most thin-film studies focus on FM materials, while little is known about AFM systems. The thickness dependence of short-period AFM CoO was found to be in accordance with Eq. (1) [12]. For Cr in Cr/Fe multilayers, on the other hand, T_N was found to decrease with d according to the empirical relation [10]

$$[T_N(\infty) - T_N(d)]/T_N(d) = C'_0 (d - d_0)^{-\lambda'}, \quad (2)$$

with a nonuniversal parameter λ' [13] and an offset

thickness $d_0 \approx 42 \text{ \AA}$ [10]. This behavior of Cr was related to a long-period incommensurate spin-density wave in combination with spin-frustration effects due to the exchange coupling with FM iron at the rough interfaces [10,11]. While $d_0 \approx 42 \text{ \AA}$ suggests a close relation to the bulk period of the spin-density wave of 60 to 78 \AA [14], the separation of the finite-size effect in these multilayers is impeded by the strong influence of the interfaces.

In order to elucidate the thickness dependence of T_N in long-period AFM thin films, we have studied thin holmium metal films with nonmagnetic interfaces, where the influence of spin frustration should be negligible. In the present Letter, we report on the results of resonant magnetic soft x-ray and neutron diffraction studies, which show that $T_N(d)$ follows Eq. (2), with the offset thickness d_0 being very close to L_b . On the basis of mean-field model calculations for free-standing thin films, we additionally give an explanation for the offset thickness d_0 and establish a linear relationship between d_0 and L_b for long-period AFM local-moment systems.

Diffraction techniques are particularly useful for the study of AFM structures, but their application to ultrathin films is rendered difficult by the tiny amount of magnetic material as well as substantial broadening of the diffraction features. Despite this, we have recently demonstrated that films of only a few ML can be studied by magnetic neutron [15] and resonant magnetic x-ray scattering at the Ho- M_V edge [16]. Particularly, the latter method provides the unprecedented sensitivity required for the thinnest films in the present study. Unpolarized neutron diffraction experiments were performed with the ADAM reflectometer at the Institut Laue-Langevin, Grenoble [17],

while resonant soft x-ray scattering experiments were carried out with linearly polarized light at the U-49/1 beam line of the Berliner Elektronenspeicherring für Synchrotronstrahlung (BESSY), using an ultrahigh-vacuum-compatible $\Theta/2\Theta$ diffractometer [16].

The experiments were carried out on two types of single-crystalline thin Ho films: One type was prepared by standard molecular-beam epitaxy (MBE) on an a-plane sapphire substrate with a Nb/Y buffer to ensure epitaxial growth and a Y/Nb cap to avoid oxidation [18]. X-ray reflectivity measurements confirmed high sample quality with a rms-roughness of the Ho/Y interfaces between two and 3 ML. The other type was grown *in situ* in ultrahigh vacuum on a W(110) substrate [16], resulting in a mean roughness of ≤ 1 ML.

Ho metal, like several of the heavy lanthanide metals [19], orders magnetically by indirect exchange between the localized $4f$ moments (RKKY interaction). Below $T_N = 131.2$ K and $T_C = 20$ K, bulk Ho metal has a helical AFM structure, with a period L_b , that changes as a function of the temperature from ≈ 7 to 12 ML [20]. The magnetic structure of bulk Ho is characterized by FM order in the basal plane of the hexagonal close-packed crystal structure. The moments of neighboring basal planes are rotated by a temperature-dependent angle ϕ , resulting in a helix along the c axis. In magnetic scattering, this gives rise to a peak at (00τ) with $\tau = c/L_b$ [15,20]. Figure 1(a) displays raw data for an 11 ML-thick MBE Ho film, recorded at $h\nu = 1353.2$ eV, which corresponds to the maximum of the M_V resonance of Ho. The square root of the integrated intensity of the (00τ) peak, which is proportional to the order parameter in the helical phase below T_N [21], is plotted as a function of T in Fig. 1(b) (solid squares). Because of pronounced short-range magnetic correlations above T_N , it is not straightforward to determine the ordering temperature from

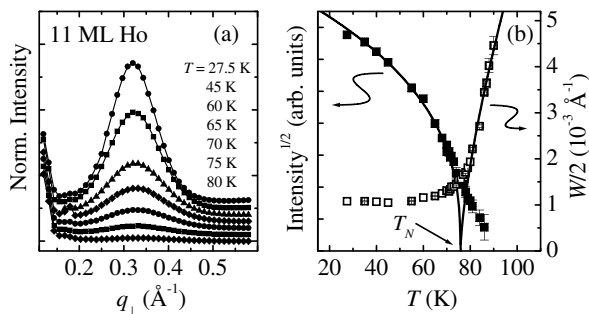


FIG. 1. (a) Magnetic structure peak (00τ) of an 11 ML-thick Ho film at various temperatures, recorded at $h\nu = 1353.2$ eV. (b) Square root of the integrated intensity of the (00τ) peak as a function of temperature (solid squares). The open squares give the half width $W/2$ of the rocking curve at (00τ) (transverse width, half width at half maximum) as a function of temperature. The solid lines represent the result of a simultaneous fit analysis.

these data alone. Therefore, we include in Fig. 1(b), shown by open squares, $W/2$ (half width at half maximum) of the corresponding rocking curves taken at (00τ) (data not shown here). In the paramagnetic phase, the (00τ) peak reflects short-range magnetic order, and $1/W$ represents the magnetic correlation length [21]. From a simultaneous power-law fit of the two data sets in Fig. 1(b), we obtain $T_N = (76 \pm 2)$ K for the 11 ML MBE film. A detailed discussion of critical scattering, however, is beyond the scope of the present Letter. Data obtained from films of various thicknesses are shown in Fig. 2, with T_N decreasing with d .

T_N as a function of d for various Ho films is shown in Fig. 3 (main panel), revealing a rather abrupt decrease around 10 ML, a behavior that had not been observed for thin films of FM Gd metal (see inset of Fig. 3). Interestingly, both types of Ho samples studied here exhibit the same thickness dependence, although they involve different interfaces. The MBE-grown Ho films are sandwiched between two Y layers with similar lattice parameters and valence-electronic structure as Ho metal. The *in situ*-grown films, on the other hand, have sharp interfaces with W(110) and vacuum, respectively, and hence should have quite different electronic structures at the interfaces. The observations therefore strongly suggest that the decrease of T_N around 10 ML is an intrinsic property of the Ho film rather than a consequence of interfaces. The best fit of Eq. (1) to the Ho data with bulk $T_N = 131.2$ K and $\lambda = 1/0.63$ [9] deviates significantly from the data (dashed line in Fig. 3). On the other hand, a very good description is obtained by fitting Eq. (2) to the data (solid line), yielding $\lambda' = 0.7 \pm 0.07$ and $d_0 = (10.8 \pm 0.5)$ ML. Thus, the magnetic behavior of thin Ho films closely resembles that of Cr [10], with a particularly interesting difference: In the Ho metal case,

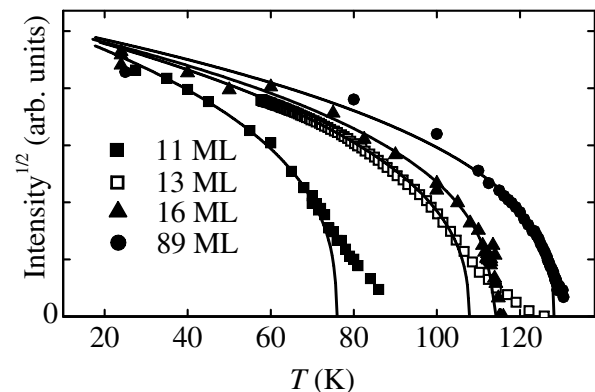


FIG. 2. Temperature dependence of the square root of the intensity of the Ho (00τ) magnetic peak for various film thicknesses d . Data were obtained from MBE films (solid squares) and from an *in situ*-grown film (open squares). Solid lines represent the results of power-law fits.

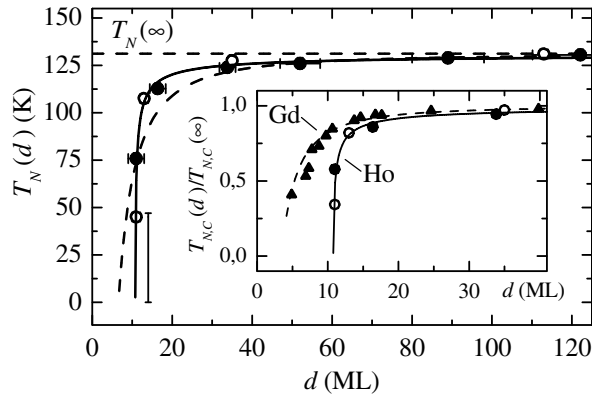


FIG. 3. T_N as a function of Ho film thickness d , including data from MBE films (solid circles) and films grown *in situ* on W(110) (open circles). The MBE films with $d \geq 16$ ML were also studied by neutron diffraction, with identical results for T_N within the error bars. For T_N of the 11 ML *in situ*-grown film, see [24]. Inset: Comparison to thin-film data for Gd (solid triangles; from Ref. [9]).

d_0 is much closer to the period of the bulk AFM superstructure than in the Cr/Fe case.

In order to understand the mechanism underlying the characteristic decrease of T_N in Ho films, we carried out mean-field calculations using a Heisenberg Hamiltonian [22]. The simplest version of this model, which reproduces the Ho magnetic structure, considers three exchange parameters J_0 , J_1 , and J_2 . $J_0 > 0$ accounts for FM coupling of the $4f$ spins within the basal plane, while J_1 and J_2 describe the coupling between nearest-neighbor and next-nearest-neighbor planes. For an infinite system at 0 K, $J_1 > 0$ and $J_2 < 0$ yield a homogeneous helical AFM structure with a constant angle ϕ between the moments of adjacent FM planes [22]:

$$\cos(\phi) = -J_1/4J_2, \quad (3)$$

provided that $|J_1/4J_2| < 1$. In order to explore the characteristics of films of finite thickness at finite temperatures T , the individual $\phi(T)$ were varied in order to minimize the free energy. Figure 4 shows the resulting magnetic ordering temperature as a function of d obtained with $J_0 = 330 \mu\text{eV}$, $J_1 = 100 \mu\text{eV}$, and $J_2 = -29 \mu\text{eV}$. For $d \rightarrow \infty$, this set of parameters leads to $T_N = 132$ K and a helix with $\phi = 30.5^\circ$, thus essentially reproducing the properties of bulk Ho. At finite d , however, *two* characteristic temperatures are found. At the higher magnetic ordering temperature (solid circles in Fig. 4), films with $d > 8$ ML order in a complex spin-block structure, which is not discussed in detail here. For $d \leq 8$ ML, this structure is FM; therefore, the higher ordering temperature is denoted by T_C . Below a second temperature T_H ($T_H < T_C$, open circles in Fig. 4), the films undergo a continuous transition to an essentially helical AFM structure, which is characterized by finite

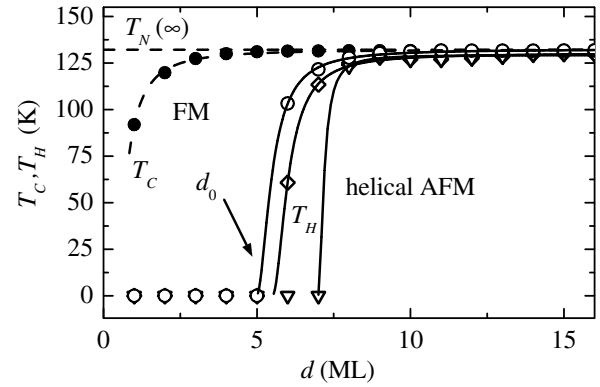


FIG. 4. Critical temperatures as a function of d , calculated within a mean-field model using various sets of exchange parameters. The dashed lines and solid lines represent fits according to Eqs. (1) and (2), respectively. For details see text.

angles $\phi(T)$. It is this latter phase that is monitored in the present scattering experiments. For $d \rightarrow \infty$, T_H can be identified with T_N , i.e., a direct transition from the paramagnetic to the helical AFM phase with no intermediate spin-block phase. Only for $d < 8$ ML, T_C and T_H are distinctly different. The thickness dependence of T_C is readily fitted by Eq. (1) (dashed line through solid circles), while T_H evidently behaves according to Eq. (2) (solid line through open circles). Fitting the theoretical data yields $\lambda = 1.85$, which is consistent with the mean-field value of $\nu = 0.5$ and $\lambda' = 1.84$, respectively.

This behavior is not limited to the J_0 - J_2 model, but is readily reproduced by other approaches. The open diamonds in Fig. 4 are obtained with a more realistic set of seven exchange parameters J_0 to J_6 as given in Ref. [23], in particular, the suppression of the helical phase for $d_0 \leq 6$ ML results. Including the six-fold in-plane crystalline anisotropy yields $d_0 = 7$ ML (open triangles), approaching the experimental $d_0 = 10.8$ ML.

One can further rationalize the existence of the offset thickness d_0 , within the J_0 - J_2 model. A more detailed inspection of the helical structure reveals a tendency of neighboring basal planes in the surface region of the film towards FM alignment, which is due to the reduced weight of the AFM next-nearest-neighbor interlayer coupling J_2 , with respect to the FM interlayer coupling J_1 . This is shown in Fig. 5(a), which displays the angles ϕ between the moments of adjacent FM planes at $T = 0$ K in the surface region. With decreasing film thickness, the surface regions become increasingly important and eventually the FM phase is favored below a film thickness equal to that of the distorted surface region (5 ML in the present calculation). The calculations further establish a close relationship between L_b and d_0 . To this end, exchange parameters were varied to yield various L_b according to Eq. (3), then d_0 was determined numerically

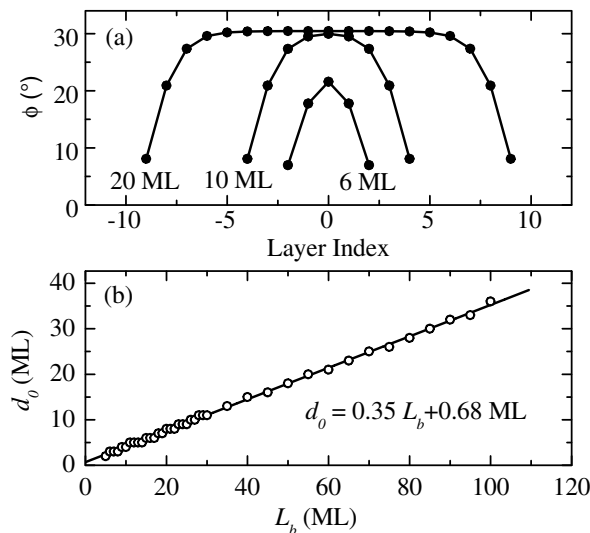


FIG. 5. Results of mean-field model calculations using J_0 - J_2 model: (a) Angle ϕ between magnetic moments of nearest neighbor planes for films with $d = 6, 10,$ and 20 ML at $T = 0$ K for fixed J_0 - J_2 . (b) Offset thickness d_0 as a function of bulk helix period L_b (see text).

using the respective J_1 and J_2 . An essentially linear relationship is obtained as shown in Fig. 5(b); the particular value of the slope is a feature of the model.

Since the present calculations were carried out for ideal freestanding films, one might question their relevance for real films. The influence of the interfaces, however, can be taken into account by allowing for layer-dependent exchange parameters in the vicinity of the interfaces. It turns out that this extension of the model towards a more realistic description of the experimental conditions does not alter the general picture, but yields just slightly changed numbers for d_0 .

In summary, the thickness dependence of the helical ordering temperature T_N of the local-moment antiferromagnet Ho metal is found to follow a modified power law with an offset thickness d_0 , similar to the case of the band AFM metal Cr. Mean-field model calculations for Ho show that d_0 depends linearly on the bulk magnetic period and is of the same order of magnitude; it represents a minimum thickness for stabilizing the long-period AFM structure. While d_0 is experimentally found to agree closely with the bulk AFM period L_b in Ho metal, it deviates considerably from L_b in the Cr/Fe case. This is interpreted as an influence of spin-frustration effects at the rough interfaces in the latter case, while the Ho metal case is dominated by the finite-size effects. The present results are expected to be of general relevance for long-period AFM structures.

The authors acknowledge the expert support and excellent beam line conditions at BESSY. The work was supported by the BMBF, Project 05KS1KEE/8, and the

DFG, Sfb-290, TPA06, and TPA01. Further support came from the BMBF under Contract No. ZA4BC2, and the Landesministerium NRW für Wissenschaft und Forschung.

*Corresponding author: eugen.weschke@physik.fu-berlin.de

†Present Address: II. Physikalisches Institut, Universität zu Köln, Zùlpicher Str. 77, D-50937 Köln, Germany.

- [1] E. L. Lee, P. E. Bolduc, and C. E. Violet, *Phys. Rev. Lett.* **13**, 800 (1964).
- [2] G. A. T. Allan, *Phys. Rev. B* **1**, 352 (1970).
- [3] M. E. Fisher and M. N. Barber, *Phys. Rev. Lett.* **28**, 1516 (1972).
- [4] C. Domb, *J. Phys. A* **6**, 1296 (1973).
- [5] H. Lutz *et al.*, *Phys. Rev. B* **18**, 3600 (1978).
- [6] Z. Q. Qiu, J. Pearson, and S. D. Bader, *Phys. Rev. Lett.* **70**, 1006 (1993).
- [7] C. M. Schneider *et al.*, *Phys. Rev. Lett.* **64**, 1059 (1990).
- [8] Yi Li and K. Baberschke, *Phys. Rev. Lett.* **68**, 1208 (1992).
- [9] M. Farle *et al.*, *Phys. Rev. B* **47**, 11 571 (1993).
- [10] E. E. Fullerton *et al.*, *Phys. Rev. Lett.* **75**, 330 (1995).
- [11] E. E. Fullerton, S. D. Bader, and J. L. Robertson, *Phys. Rev. Lett.* **77**, 1382 (1996).
- [12] T. Ambrose and C. L. Chien, *Phys. Rev. Lett.* **76**, 1743 (1996).
- [13] Renjun Zhang and Roy F. Willis, *Phys. Rev. Lett.* **86**, 2665 (2001).
- [14] E. Fawcett, *Rev. Mod. Phys.* **60**, 209 (1988).
- [15] V. Leiner *et al.*, *Physica B (Amsterdam)* **283**, 167 (2000).
- [16] C. Schùbler-Langeheine *et al.*, *J. Electron Spectrosc. Relat. Phenom.* **114-116**, 953 (2001).
- [17] See <http://www.ill.fr/YellowBook/ADAM>.
- [18] J. Kwo, in *Thin Film Techniques for Low-Dimensional Structure*, edited by R. F. C. Farrow, S. S. P. Parkin, P. J. Dobson, N. H. Neaves, and A. S. Arrott, NATO ASI Ser. B Vol. 13 (Plenum, New York, 1988).
- [19] W. C. Koehler, in *Magnetic Properties of Rare Earth Metals*, edited by R. J. Elliott (Plenum, London, 1972), Vol. 10, p. 81.
- [20] M. J. Pechan and C. Stassis, *J. Appl. Phys.* **55**, 1900 (1984).
- [21] G. Helgesen *et al.*, *Phys. Rev. B* **50**, 2990 (1994).
- [22] B. Coqblin, *The Electronic Structure of Rare-Earth Metals and Alloys: The Heavy Magnetic Rare Earths*, (Academic Press, London 1977), Chap. 3.
- [23] J. Bohr *et al.*, *Physica B (Amsterdam)* **159**, 93 (1989).
- [24] For 11 ML Ho/W(110), no magnetic peak was observed down to the lowest available temperature (45 K). Therefore, T_N is located between 0 K and 45 K, as indicated by the separately shown error bar. The difference to the 11 ML MBE film is readily explained by a slightly different thickness within the error bar of d , since $T_N(d)$ depends very sensitively on d in this thickness range.